AD-A144 824   EXPERIMENTAL PROPERTIES OF AN INHOMOGENEOUSLY BROADENED   1/1
                HE-XE UNSTABLE RING LASER(U) AIR FORCE WEAPONS LAB
                KIRTLAND AFB NM   Y M LIU   JUL 84   AFWL-TR-84-30
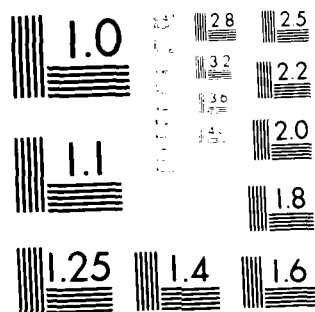UNCLASSIFIED   F/G 20/5   NL

END
DATE
FILMED
9-84
DTIC

‖‖ 1.0 ‖‖ 2.8 ‖‖ 2.5
         ‖‖ 3.2 ‖‖ 2.2
         ‖ 3.6
         ‖‖   ‖‖ 2.0

‖‖ 1.1   ‖‖ 1.8

‖‖ 1.25 ‖‖ 1.4 ‖‖ 1.6

MICROCOPY RESOLUTION TEST CHART

②

EXPERIMENTAL PROPERTIES
OF AN INHOMOGENEOUSLY BROADENED
He-Xe UNSTABLE RING LASER

Ying-Moh Liu

AD-A144 824

July 1984

Final Report

Approved for public release; distribution unlimited.

DTIC
ELECTE
AUG 2 4 1984

B

AIR FORCE WEAPONS LABORATORY
Air Force Systems Command
Kirtland Air Force Base, NM   87117

8   004

This final report was prepared by the Air Force Weapons Laboratory, Kirtland Air Force Base, New Mexico, under Job Order ILIR8203. Dr. Christopher M. Clayton (ARAO) was the Laboratory Project Officer-in-Charge.

When Government drawings, specifications, or other data are used for any purpose other than in connection with a definitely Government-related procurement, the United States Government incurs no responsibility or any obligation whatsoever. The fact that the Government may have formulated or in any way supplied the said drawings, specifications, or other data, is not to be regarded by implication, or otherwise in any manner construed, as licensing the holder, or any other person or corporation; or conveying any rights or permission to manufacture, use, or sell any patented invention that may in any way be related thereto.

This report has been authored by an employee of the United States Government. Accordingly, the United States Government retains a nonexclusive, royalty-free license to publish or reproduce the material contained herein, or allow others to do so, for the United States Government purposes.

This report has been reviewed by the Public Affairs Office and is releasable to the National Technical Information Services (NTIS). At NTIS, it will be available to the general public, including foreign nations.

If your address has changed, if you wish to be removed from our mailing list, or if your organization no longer employs the addressee, please notify AFWL/ARAO, Kirtland AFB, NM 87117 to help us maintain a current mailing list.

This technical report has been reviewed and is approved for publication.

CHRISTOPHER M. CLAYTON
Project Officer

FOR THE COMMANDER

JAMES W. MAYO III   DAVID W. SEEGMILLER
Lt Colonel, USAF   Colonel, USAF
Chief, Advanced Resonator/Optics Br   Chief, Advanced Laser Technology Div

REPORT DOCUMENTATION PAGE

1a. REPORT SECURITY CLASSIFICATION		1b. RESTRICTIVE MARKINGS		
Unclassified				
2a. SECURITY CLASSIFICATION AUTHORITY		3. DISTRIBUTION/AVAILABILITY OF REPORT		
		Approved for public release; distribution unlimited.		
2b. DECLASSIFICATION/DOWNGRADING SCHEDULE				
4. PERFORMING ORGANIZATION REPORT NUMBER(S)		5. MONITORING ORGANIZATION REPORT NUMBER(S)		
AFWL-TR-84-30				
6a. NAME OF PERFORMING ORGANIZATION	6b. OFFICE SYMBOL (If applicable)	7a. NAME OF MONITORING ORGANIZATION		
Air Force Weapons Laboratory	ARAO			
6c. ADDRESS (City, State and ZIP Code)		7b. ADDRESS (City, State and ZIP Code)		
Kirtland Air Force Base, NM 87117				
8a. NAME OF FUNDING/SPONSORING ORGANIZATION	8b. OFFICE SYMBOL (If applicable)	9. PROCUREMENT INSTRUMENT IDENTIFICATION NUMBER		
8c. ADDRESS (City, State and ZIP Code)		10. SOURCE OF FUNDING NOS.		

	PROGRAM ELEMENT NO.	PROJECT NO.	TASK NO.	WORK UNIT NO.
	61101F	ILIR	82	03

11. TITLE (Include Security Classification)
EXPERIMENTAL PROPERTIES OF AN INHOMOGENEOUSLY BROADENED He-Xe UNSTABLE RING LASER (U)

12. PERSONAL AUTHOR(S)
Ying-Moh Liu

13a. TYPE OF REPORT	13b. TIME COVERED		14. DATE OF REPORT (Yr., Mo., Day)	15. PAGE COUNT
Final Report	FROM Oct 81 TO Dec 83		1984 July	50

16. SUPPLEMENTARY NOTATION

17. COSATI CODES			18. SUBJECT TERMS (Continue on reverse if necessary and identify by block number)
FIELD	GROUP	SUB. GR.	Helium Xenon Laser, Doppler-Broadened Gain Medium, Ring Resonators, Longitudinal Mode Competition, Reverse Mode Suppression
20	05		

19. ABSTRACT (Continue on reverse if necessary and identify by block number)

Although the ring resonator has been previously investigated in several ways, the unstable ring resonator with inhomogeneously broadened gain medium is not yet well understood.

The objective of this thesis is to explore reverse mode suppression in an unstable ring resonator by using a helium-xenon (He-Xe) gas mixture which is inhomogeneously broadened. The optical feedback technique employing a suppressor mirror was used. Several aspects of the unstable ring resonator are discussed: the relative power levels in forward and reverse waves, with and without the suppressor mirror, with strong and weak couplings from reverse wave to forward wave; the near field and far field patterns; and the mode volume effect. The degree of suppression in the reverse wave and the degree of increase in the forward wave, when the suppressor mirror was in place, are also discussed.

20. DISTRIBUTION/AVAILABILITY OF ABSTRACT	21. ABSTRACT SECURITY CLASSIFICATION	
UNCLASSIFIED/UNLIMITED ☒ SAME AS RPT. ☐ DTIC USERS ☐	Unclassified	
22a. NAME OF RESPONSIBLE INDIVIDUAL	22b. TELEPHONE NUMBER (Include Area Code)	22c. OFFICE SYMBOL
Dr. C. M. Clayton	(505) 844-4597	ARAO

DD FORM 1473, 83 APR   EDITION OF 1 JAN 73 IS OBSOLETE.

i

This thesis is dedicated to my parents.

iii

ACKNOWLEDGMENTS

EXPERIMENTAL PROPERTIES OF AN INHOMOGENEOUSLY

BROADENED He-Xe UNSTABLE RING LASER

BY

YING-MOH LIU

ABSTRACT OF THESIS

Submitted in Partial Fulfillment of the
Requirements for the Degree of

Master of Science in Engineering

The University of New Mexico
Albuquerque, New Mexico
December, 1983

EXPERIMENTAL PROPERTIES OF AN INHOMOGENEOUSLY
BROADENED He-Xe UNSTABLE RING LASER

Ying-Moh Liu

B.S., National Chiao-Tung University, 1978

Although the ring resonator has been previously investigated in several ways, the unstable ring resonator with inhomogeneously broadened gain medium is not yet well understood.

The objective of this thesis is to explore reverse mode suppression in an unstable ring resonator by using a helium-xenon (He-Xe) gas mixture which is inhomogeneously broadened. The optical feedback technique employing a suppressor mirror was used. Several aspects of the unstable ring resonator are discussed: the relative power levels in forward and reverse waves, with and without the suppressor mirror, with strong and weak couplings from reverse wave to forward wave; the near field and far field patterns; and the mode volume effect. The degree of suppression in the reverse wave and the degree of increase in the forward wave, when the suppressor mirror was in place, are also discussed.

TABLE OF CONTENTS

LIST OF FIGURES

TABLE

CHAPTER I

INTRODUCTION

Although the ring resonator has been investigated in several ways, the unstable ring resonator with inhomogeneously broadened gain medium has not been fully explored. The reverse mode suppression in a homogeneously broadened gain medium was investigated by Freiberg utilizing a suppression mirror. In both of Freiberg's studies, the gain medium was carbon-dioxide (CO_2) which was homogeneously broadened.

The objective of this thesis is to explore reverse wave suppression in an unstable ring resonator using a helium-xenon (He-Xe) gas mixture which is inhomogeneously broadened. The laser wavelength was 3.5 μm. During the experiment, the optical feedback technique of reverse mode suppression was examined. Several measurements were taken:

(1) measurement of the relative power levels in forward and reverse waves with and without suppressor mirror;

(2) measurement of relative power levels in forward and reverse wave with strong and weak coupling from reverse wave to forward wave.

A comparison of the in-plane configuration and the off-plane configuration for the elimination of astigmatism was also studied. Near field and far field pictures were taken. The Doppler-broadened medium effect on the mode spectra is also discussed.

1.1. History

The advantages of the unstable resonator were first pointed out by Siegman in 1965 [1]. He pointed out that the diffraction losses for practical unstable resonators may be useful for transverse mode control. Since then, the unstable resonator has found extensive use in many high energy lasers, for instance, carbon dioxide, carbon monoxide, hydrogen fluoride, krypton fluoride. A tutorial review of the unstable resonators is given by Steier [2].

The concept of a laser employing an unstable ring resonator geometry was first discussed in literature by Anan'ev in 1969 [3]. Since that time, Freiberg [4] has done extensive studies on the unstable ring resonator. He used a carbon dioxide laser gas mixture as the gain medium, which was homogeneously broadened. In his later studies [5,6], he investigated the reverse mode suppression by either employing a mode volume discrimination scheme, or using a suppressor mirror. In both cases, Freiberg [5,6] used a carbon dioxide gain medium.

A stable ring resonator with inhomogeneously broadened helium-neon gas mixture was investigated by F. R. Faxvog [7,8]. Although these studies have been performed on unstable homogeneously broadened ring lasers and on stable inhomogeneously broadened ring lasers, the properties of the inhomogeneously broadened unstable ring laser have not previously been obtained. Such research will improve the current understanding of ring laser physics.

1.2. The Advantages of the Unstable Resonator

Stable resonators have several important limitations. For stable resonators, a low gain lasing medium can be used. Since the light rays of a laser mode are trapped between the surfaces of the resonator mirrors, rays do not walk out past their edges. The output from the laser is transmitted through a partially transmitting mirror. To produce a diffraction-limited output beam, the Fresnel number, or the number of Fresnel zones in the limiting aperture of the laser must be on the order of unity or smaller, which usually limits the diameter of the laser gain medium to a few millimeters. These factors, the transmissive optical elements, the low Fresnel number, and the small gain region diameter, all limit the applications of stable resonators, so it is important to study unstable resonators.

The unstable resonators frequently can offer better performance. For a laser system characterized by at least moderate growth or amplification per pass (50% per pass) and by a Fresnel number greater than unity, the preferred laser cavity will usually be an unstable resonator. For any such laser system, at any power level, provided only that the optical quality of the laser medium itself is not extremely poor, the unstable resonator provides the most practical method for obtaining nearly complete energy extraction from the laser medium, combined with high beam quality. Hence, the unstable resonator is a good candidate in many applications.

In general, as presented by Siegman [9], unstable resonators have several advantages:

1. Unstable resonators can have a large mode volume even in a
short resonator.

2. The unstable configuration can be readily adapted to
adjustable diffraction output coupling.

3. Analysis indicates that unstable resonators have substan-
tial discrimination against higher order transverse modes.

4. Unstable resonators usually use reflective optics only,
which have less stringent laser damage requirements than
the transmissive optics which are used in conventional
stable resonators.

In summary, the principal drawback of the unstable resonator is
that it can only be employed with high gain lasing media, while a low
gain medium can be used in a stable resonator. However, the unstable
resonator is superior to the stable resonator for many applications, so
it is important to develop an understanding of its properties.

Unstable resonators can be divided into two classes: the
standing-wave unstable resonators and the traveling-wave unstable
resonator, or the unstable ring resonator. Although the standing-wave
unstable resonator has many applications, the unstable ring resonator
has certain advantages. A discussion follows in the next section.

1.3. Advantages of Unstable Ring Resonator

In contrast to unstable standing-wave resonators, the unstable
ring resonator can support two weakly coupled intracavity traveling
waves of different mode diameters which propagate in opposite
directions within the ring geometry.

Ring resonators are of interest for several reasons:

(1) In unstable standing-wave resonators, there are necessarily two traveling waves going in the positive and negative Z directions simultaneously. In a ring resonator, by using the mode volume discrimination scheme or by using a suppressor mirror to suppress the reverse wave, a unidirectional traveling wave can be obtained.

(2) An unstable standing-wave resonator with a long gain region usually requires a long radius mirror as a feedback mirror, which makes it difficult to have good mode control. In an asymmetric unstable ring resonator, which will be discussed in more detail, there is greater design flexibility to use shorter radius mirrors, which makes the resonators easier to align and causes them to be less sensitive to wavefront aberrations introduced by the gain medium.

(3) In unidirectional ring resonators, it is easier to correct wave aberrations by using adaptive optics (for example, deformable mirrors) than it is in standing-wave resonators.

Since unstable ring resonators have the advantages discussed above, a detailed study of their properties is an important contribution to the field of laser physics.

CHAPTER II

THEORY

The basic ring resonator theory, including the definitions of
terms, will be given in section 2.1 of this chapter. The theory of
reverse mode suppression, which is the main subject of this thesis,
will be discussed in detail in section 2.2. The mode competition in a
Doppler-broadened medium will be discussed in section 2.3. In section
2.4, the geometric properties of the forward and reverse waves,
including the beam diameters at several apertures, and the mode volumes
over the gain region, are derived and given.

2.1. Basic Resonator Theory

Before explaining resonator theory, some terms must be defined.
As the confocal ring resonator will be discussed throughout the entire
thesis, the confocal ring resonator is defined first. Positive and
negative branch confocal rings, and symmetric and asymmetric confocal
rings will also be defined.

As shown in Fig. 1 and Fig. 2, the confocal ring resonator
contains a confocal telescope in the ring. "Confocal" means the focal
points of the two curved mirrors in the ring are coincident.

Resonators, both stable and unstable, are usually described in
terms of two parameters g_1 and g_2:

$$g_1 = 1 - (L/R_1), \quad g_2 = 1 - (L/R_2) \tag{1}$$
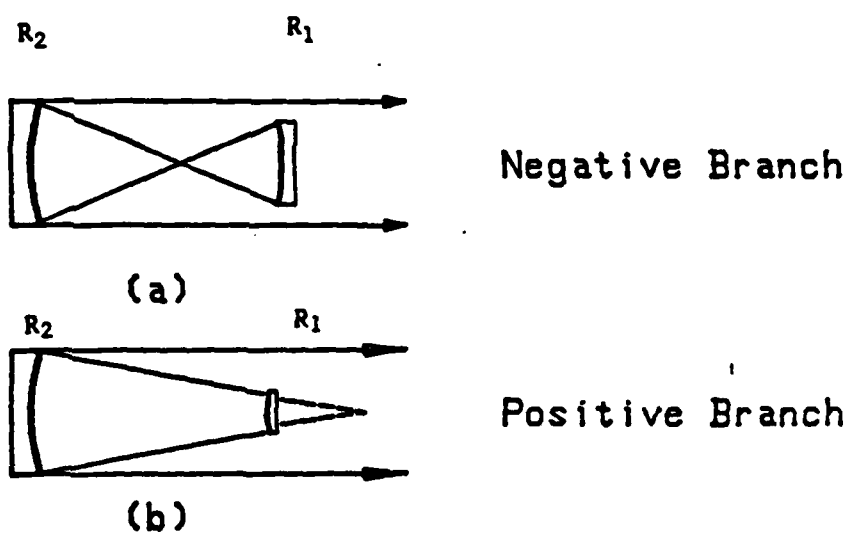
Negative Branch

(a)

Positive Branch

(b)

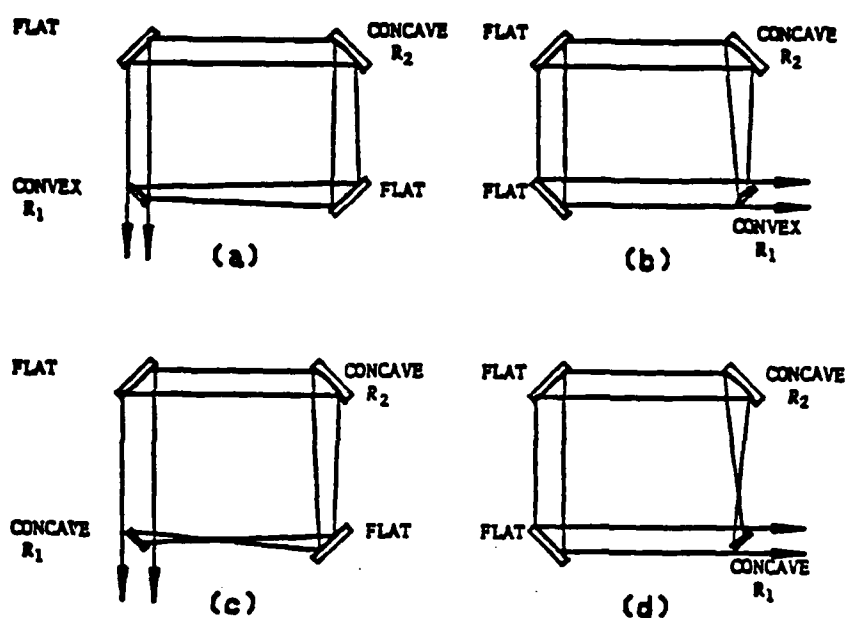Figure 1. Diagram of positive and negative branch confocal unstable
resonators.

Figure 2. Ring resonator configurations.

(a) Positive branch, symmetric ring resonator,
(b) positive branch, asymmetric ring resonator,
(c) negative branch, symmetric ring resonator,
(d) negative branch, asymmetric ring resonator.

where L is the spacing between the curved mirrors in stable

resonators or unstable standing-wave resonators. For

unstable ring resonators, L is the perimeter of the

ring. R_1 and R_2 are the radii of curvature of the

curved mirrors.

R_1, R_2 = radii of curvature of the mirrors (R_1 and R_2 are

positive for concave mirrors).

Stable resonators satisfy the condition:

$$0 < g_1 g_2 < 1 \qquad (2)$$

Unstable resonators satisfy the condition:

$$g_1 g_2 < 0 \text{ or } g_1 g_2 > 1 \qquad (3)$$

For a confocal ring, if $g_1 < 0$ and $g_2 < 0$, then it is a
negative branch resonator; if $g_1 > 0$ and $g_2 > 0$, then it is a positive
branch resonator. A negative branch confocal ring resonator always has
an intracavity focus, which may make it undesirable for high power
lasers.

The positive-branch symmetric ring is shown in Fig. 2(a); its
asymmetric analog is shown in Fig. 2(b). Figures 2(c) and 2(d) are the
negative-branch counterparts of Figs. 2(a) and 2(b), respectively.
These figures clearly show the difference between the two rings. Both
the symmetric and asymmetric ring resonators have two parts, that is,
the uncollimated part goes counterclockwise from R_1 to R_2, and the

collimated part covers the rest of the ring. However, the main

difference between the symmetric and asymmetric resonator is that the

collimated and the uncollimated parts of a symmetric resonator have

equal lengths, while the collimated and uncollimated parts of an

asymmetric resonator have different lengths. The name "symmetric ring

resonator" derives from the property that at a given distance from the

scraper mirror in the counterclockwise (CCW) direction, the forward

beam is the same as the reverse beam at that distance from the scraper

mirror in the clockwise (CW) direction.

2.2. Theory of Reverse Mode Suppression

A ring resonator can sustain two traveling waves going in

opposite directions. Only the forward out-coupled wave is useful. The

reverse wave competes with the forward wave for the laser gain, and in

some instances it may cause unacceptable thermal loading on optical

elements. Hence, suppression of the reverse wave is usually desirable.

It is possible to suppress the reverse wave of an asymmetric

confocal ring laser by making use of the principle that the reverse

wave is not collimated anywhere in the resonator. Therefore, the gain

cell can be put over a section where the ratio of the forward wave mode

volume (V_F) to the reverse mode volume (V_R) is the largest to maximize

the ratio of the forward wave power (P_F) to the reverse power (P_R).

This principle can be understood easily by looking at Fig. 3.

In addition to the mode volume difference between forward and

reverse waves, another technique is to employ a suppressor mirror which

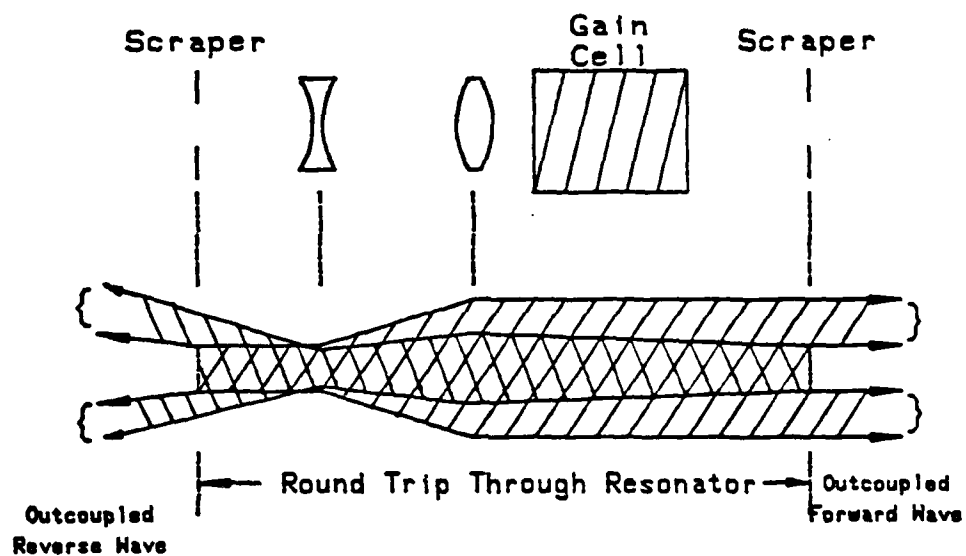is illustrated in Fig. 4. The reverse wave first gets scraped out by

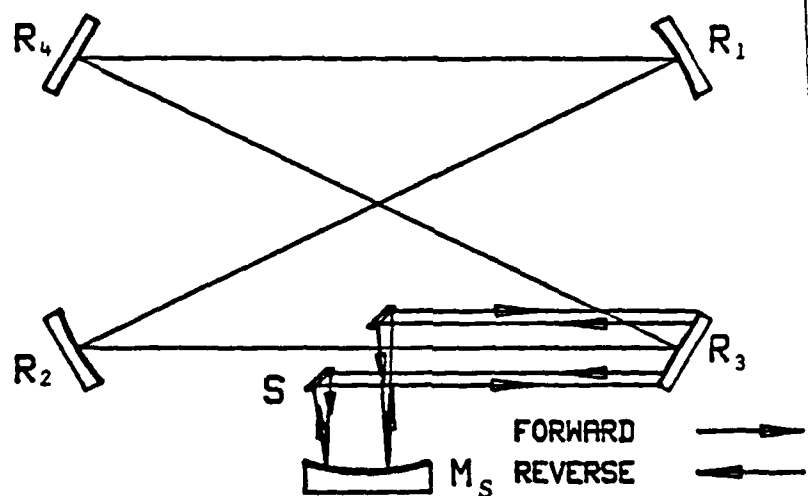Figure 3. The comparison of forward and reverse mode volumes.

Figure 4. The function of the suppressor mirror.

the scraper mirror (S), hits the suppressor mirror (M_S), is reflected back to the scraper mirror, and then is reflected back into the forward direction. Hence, during the buildup of the fields, the forward wave will grow faster because of the contribution from the feedback of the reverse wave. This effect will enhance the reverse wave suppression caused by the mode volume difference.

The effect of the suppressor mirror sends the reverse wave into the forward direction, and mode matches the reflected reverse wave with the forward wave. Since the outcoupled wave in the forward direction is collimated, the mode matching consideration requires that the returned portion of the reverse wave must also be collimated. Hence, both the location and the radius of the suppressor mirror would affect the radius of curvature of the wavefront of the feedback reverse wave. However, according to Freiberg's [6] experimental data, the reverse mode suppression is not unduly sensitive to mirror curvature and location.

In summary, it is desirable to do an investigation of reverse wave suppression. Suppression can be obtained by using the mode volume discrimination technique, and then enhanced by employing a suppressor mirror.

2.3. Mode Competition in a Doppler-Broadened Medium

Mode competition has a significant effect on the mode spectrum. A discussion of the effects of a Doppler-broadened medium on the forward and reverse mode spectra, and on the reverse wave suppression is given in this section.

A mathematical treatment of the mode spectra is given here. For a ring laser, in the forward direction, the resonance condition is

$$kv = \omega_1 - \omega_0 \tag{4}$$

where v = velocity of atoms,

ω_0 is the center frequency of the gain curve, and

ω_1 is the laser cavity mode frequency.
For the reverse wave,

$$kv = \omega_0 - \omega_1' \tag{5}$$

where ω_1' is the laser cavity frequency in the reverse direction. Hence, there are two modes in either direction competing with the same velocity group of atoms, one on either side of ω_0.

Mirror modes are two modes with frequencies ω_1, $\omega_2(\omega_2 > \omega_1)$ satisfying $\omega_2 \approx 2\omega_0 - \omega_1$, where ω_0 is the center frequency of the gain curve. Since a pair of oppositely traveling mirror modes are resonant with the same atoms, it is to be expected that the mode with lower loss will tend to suppress the other.

The effect of the suppressor mirror may be included in a set of $2n$ coupled integrodifferential laser rate equations:

$$\frac{dI_i^+}{d\tau} = \left(\frac{G_i^+}{G_0} - \frac{G_T}{G_0}\right) I_i^+ + \frac{I_i^- r}{G_0 L}$$

$$\frac{dI_i^-}{d\tau} = \left(\frac{G_i^-}{G_0} - \frac{G_T}{G_0}\right) I_i^- + \frac{I_i^+ r'}{G_0 L}$$

(6)

where

I_i^+ is the intensity of the i-th forward mode,

I_i^- is the intensity of the i-th reverse mode,

$\tau = G_0 c t$,

$G_0 = B n_0 / \sqrt{\pi} \, \Delta$

= line-center small-signal gain in the Doppler limit

$G_i^\pm$ = total gain per unit length in the forward direction (denoted "+") and reverse direction (denoted "-").

$$= \int g_i^\pm \, d\nu$$

and

$g_i^\pm \, d\nu$ = the gain due to a group of molecules with velocity between v and $v + dv$

$$= \frac{B n_0 W(\nu) L_i^\pm \, d\nu}{1 + \frac{B}{\gamma \hbar \omega_0} \sum_i (I_i^+ L_i^+ + I_i^- L_i^-)}$$

(7)

where

$\nu = kv$

$$\gamma = \text{decay rate}$$

$$w(\nu) = \frac{1}{\sqrt{\pi}\Delta} \exp[-(\frac{\nu}{\Delta})^2]$$

$$\Delta = \text{half-width of Doppler distribution to } \frac{1}{e} \text{ point}$$

$$L_i^{\pm} = \text{Doppler-shifted Lorentzian resonance shape}$$

$$= \frac{\beta}{\pi[\beta^2 + (\omega_i - \omega_0 \mp \nu)^2]} \tag{8}$$

$$\beta = \text{homogeneous width}$$

In the coupled equations, a phenomenological coupling constant, r, is introduced to represent the coupling from the reverse modes into the forward modes; this coupling constant includes the effect of a reverse mode suppressor mirror. Similarly, r' is introduced to represent the coupling from the forward modes into the reverse modes due to processes such as scattering from mirror surfaces and reflection from windows.

Mode spectra of forward and reverse waves in a stable helium-neon ring laser were studied by Faxvog [8], who found that some configurations of Doppler-broadened ring lasers, with suppressor mirrors, had longitudinal mode distributions that were symmetric with respect to line center. By assuming a symmetric intensity distribution, the steady-state forward and reverse intensities can be obtained by taking

$$\frac{d}{d\tau} I_i^+ = \frac{d}{d\tau} I_i^- = 0 . \tag{9}$$

Using Eqs. (11) and (8) their ratio is

$$\frac{I_i^+}{I_i^-} = \sqrt{\frac{r}{r'}} \tag{10}$$

i.e.,

$$\frac{\text{Forward Intensity}}{\text{Reverse Intensity}} = \left[\frac{\text{Reverse} \rightarrow \text{Forward Coupling}}{\text{Forward} \rightarrow \text{Reverse Coupling}}\right]^{\frac{1}{2}}$$

Numerical studies of both steady-state mode spectra and time-dependent intensities of forward and reverse modes for several cases have been done by A. H. Paxton [11]. When the calculation was started with an initial intensity distribution that was symmetric with respect to line center, a symmetric steady-state intensity mode distribution would result. When an initial mode distribution with most of its power in the modes with frequency on one side of line center was assumed, a steady-state solution with most of its power in modes with frequency on the same side of line center would result.

The foward and reverse mode spectra depend on both the coupling constants, from Faxvog's study [8], and the initial conditions of the modal intensity distribution, from Paxton's [11] study. Asymmetric mode spectra might not be desirable, since it might cause severe transverse mode control problems. Previous work has indicated complicated behavior in Doppler-broadened ring lasers, and this work is aimed at clarifying this problem.

2.4. Geometric Properties of Forward and Reverse Modes

A study of the geometric properties leads to the understanding of the mode volume discrimination effect. The mode diameters, at several apertures in the ring, of forward and reverse waves are calculated in this section. The mode volumes of the forward and reverse waves within the gain region are also calculated.

Figure 5 shows an unfolded ring, with the reverse wave moving in the positive z direction. Point c on the z-axis represents the center of curvature of the reverse wave; S represents the scraper with inner hole radius a_1; the rectangular box represents the gain cell having reverse beam radii a_4 and a_5 on each end; f_2 and f_1 represent the two curved mirrors, which have beam radii a_2 and a_3, respectively.

To derive the mode volumes, several distances, d_2, d_3, d_4 need to be determined in terms of the known factors.

M = magnification = f_2/f_1

$L_1 = f_1 + f_2 = f_1 + Mf_1 = (M+1)f_1$

$f_1 = L_1/(M+1)$

$f_2 = ML_1/(M+1)$

From the lens equation associated with f_2,

$$\frac{1}{d_1 + L_3} + \frac{1}{d_2} = \frac{1}{f_2} = \frac{M+1}{ML_1}$$
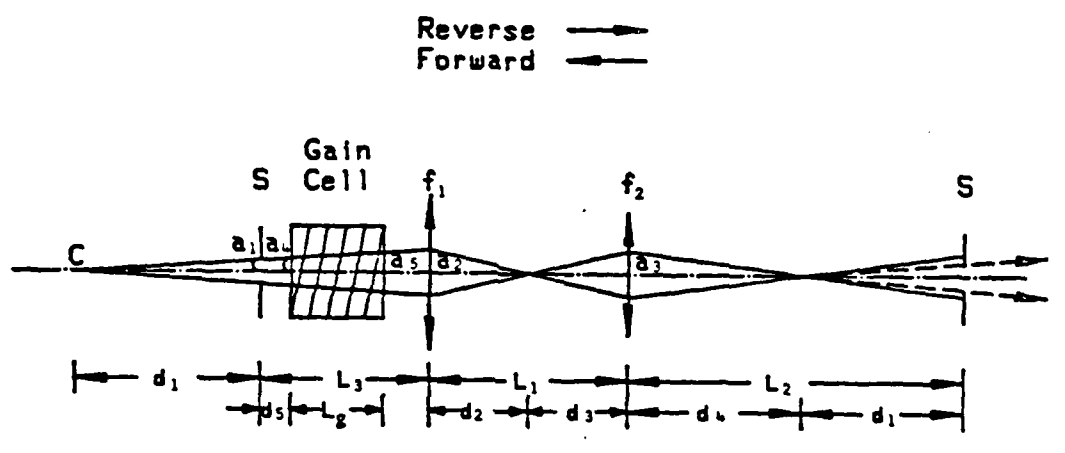
(11)

d_2 can be deduced with

Figure 5. Geometric properties of forward and reverse waves.

(For convenience in labeling, a focus is shown between f_2 and S. The distance d_4 is actually negative and no focus exists in this leg of the resonator.)

$$d_2 = \frac{(d_1 + L_3)L_1 M}{(d_1 + L_3)(M + 1) - L_1 M} \quad , \tag{12}$$

and

$$d_3 = L_1 - d_2 \tag{13}$$

$$= \frac{L_1(d_1 + L_3 - L_1 M)}{(d_1 + L_3)(M + 1) - L_1 M} \quad .$$

From the lens equation associated with f_1,

$$\frac{1}{d_3} + \frac{1}{d_4} = \frac{1}{f_1} = \frac{M + 1}{L_1} \quad , \tag{14}$$

and d_4 can be deduced to be

$$d_4 = \frac{-d_1 - L_3 + L_1 M}{M^2} \tag{15}$$

Hence d_2, d_3, d_4 are expressed in terms of the known factors M, L_1, L_3 and an unknown d_1. However, this unknown factor d_1 can be deduced from the self-consistency requirement that the center of curvature of the reverse wave stays at the same relative position to the scraper after one round trip, hence

$$L_2 - d_4 = d_1 \tag{16}$$

i.e.,

$$L_2 + \frac{d_1 + L_3 - L_1 M}{M^2} = d_1, \tag{17}$$

and d_1 can be expressed in terms of L_1, L_2, L_3, which are in turn determined by the equivalent Frensel number consideration, and M.

The beam sizes on the two mirrors can be obtained by using a similar triangle relationship,

$$\frac{a_1}{d_1} = \frac{a_2}{d_1 + L_3} \tag{18}$$

obtaining

$$a_2 = \frac{a_1(d_1 + L_3)}{d_1}$$

$$= \frac{a_1[(L_2 + L_3)M^2 - L_1 M]}{L_2 M^2 - L_1 M + L_3} . \tag{19}$$

Also,

$$\frac{a_3}{a_2} = \frac{d_3}{d_2} \tag{20}$$

obtaining

$$a_3 = \frac{a_2 d_3}{d_2} = a_1 M \frac{L_2 + L_3 - L_1 M}{L_2 M^2 - L_1 M + L_3} \tag{21}$$

Hence, beam sizes a_2, a_3 are expressed in terms of the known factors M, L_1, L_2, L_3 and a_1.

In the experimental setup, which had

$$a_1 = 1 \text{ cm}, \qquad M = 1.33, \qquad L_1 = 350 \text{ cm},$$

$$L_2 = 217 \text{ cm}, \qquad L_3 = 579 \text{ cm},$$

a_2 and a_3 are obtained, for the reverse wave, as

$$a_2 = 1.98 \text{ cm}$$

$$a_3 = 0.88 \text{ cm}.$$

The forward mode volume, V_F is

$$V_F = \pi (a_1 M)^2 L_g \tag{22}$$

where

$a_1 M$ = radius of forward mode at the gain cell,

L_g = length of gain cell

= 124 cm,

thus

$$V_F = 688.7 \text{ cm}^3.$$

In the reverse direction, d is obtained as

$$d_1 = 646.8 \text{ cm}.$$

From similar triangle relationships,

$$\frac{a_1}{d_1} = \frac{a_4}{d_1 + d_5} \quad , \tag{23}$$

and

$$\frac{a_1}{d_1} = \frac{a_5}{d_1 + d_5 + L_g} \quad . \tag{24}$$

with $d_5 = 400$ cm, a_4 and a_5 can be calculated out as

$$a_4 = 1.62 \text{ cm}, \qquad a_5 = 1.81 \text{ cm}$$

the reverse mode volume can be obtained by

$$V_R = \frac{1}{3} \pi [a_5^2(d_1 + d_5 + L_g) - a_4^2(d_1 + d_5)]$$

$$= 1139.2 \text{ cm}^3 \quad . \tag{25}$$

The reverse mode volume is much greater than the forward mode volume. This result is contrary to the desire to have a greater forward mode volume, to achieve reverse mode suppression by the mode volume discrimination technique. However, the experimental data still showed a greater forward wave power. An explanation of the data can be deduced from the experimental result of Klüver [10], who obtained a higher gain in the central region than near the walls of a gain cell, which had a helium-xenon gain medium running at 3.5 μm. A fuller explanation will be given in Chapter III, section 3.4.4.

CHAPTER III

EXPERIMENT

The experiment used a Doppler-broadened helium-xenon gas mixture as the gain medium. The reverse wave suppression phenomenon was investigated in the experiment, which employed an unstable asymmetric ring resonator.

The basic properties of an unstable asymmetric ring resonator were discussed in the preceeding chapters. This chapter contains discussions of: the experimental set-up in section 3.1; the experimental concerns in section 3.2; the optical design in section 3.3; and experimental results in section 3.4, including the measured power levels in forward and reverse waves, with and without suppressor mirror, and with strong and weak couplings from reverse wave to forward wave. Near field and far field patterns of the forward and reverse waves for both in-plane and off-plane configurations will be examined.

3.1. The Experimental Setup

The basic structure of the experiment was an unstable asymmetric ring resonator. The initial resonator was an in-plane configuration as shown in Fig. 6. The optical system design was based on two considerations:
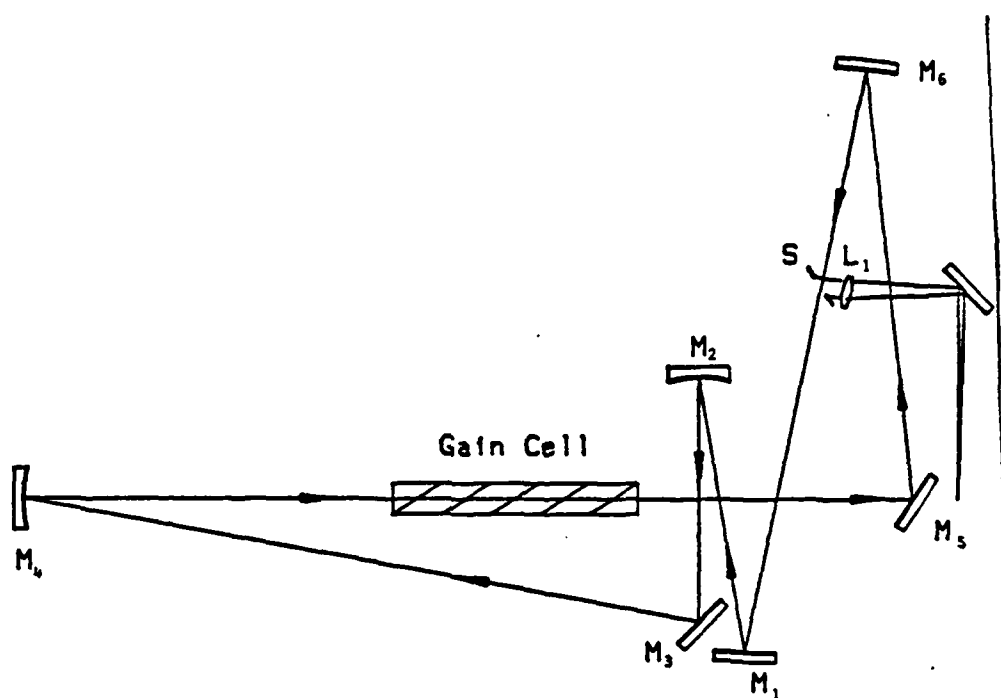
Figure 6. Layout of in-plane configuration.

(1) Minimal aberration — minimizing aberrations by keeping
the incidence angles on the two curved mirrors small while
simultaneously staying in plane, and fitting into the
available table space;

(2) half integer equivalent Fresnel number — arranging the
distances between mirrors to obtain a half-integer
equivalent Fresnel number.

The in-plane unstable ring resonator was rather complex. It
contained seven intracavity mirrors, as shown in Fig. 6. The arrows in
this figure also show the forward beam's path. The forward direction
is defined from M_2 to M_4. The light ray in the forward direction
starts from the scraper (S), then hits the flat mirror M_1, and follows
the path indicated by the arrows until it returns to the scraper. This
path is a round trip pass. Although most of the mirrors in the
resonator were planar, two mirrors, M_2 and M_4, had a concave shape; M_2
had a 3-meter radius, while M_4 had a 4-meter radius. M_2 and M_4 formed
a confocal telescope, inside the resonator, which collimated the
forward wave, and gave a 1.33 geometric magnification. The collimated
forward out-coupled beam was then focused by a positive lens, L_1, with
100 cm focal length for power measurement and mode spectrum analysis.
This completes the description of the basic structure of the in-plane
configuration.

The degree of aberration is an important assessment of a laser
system. Since the in-plane scheme resulted in a severe astigmatism in
the forward wave, an off-plane configuration as shown in Fig. 7 was
employed. As Fig. 7 shows, the forward beam follows a path indicated

Figure 7. Layout of off-plane configuration.

by the arrows. The beam moves away from the table between M_6 and M_1; during the transit it passes through the scrapers S_1 and S_2. The beam travels downward toward the table between M_1 and M_2 with an angle of $4.5°$. All of the components were in the same plane except the scrapers S_1, S_2 and the plane mirror M_1, which were placed higher. The gain cell is shown as a cross-hatched rectangle in Fig. 7.

The sizes of the mirrors were not the same. Referring to Fig. 7, most of the mirrors had 6" diameter, except M_1 had 3" diameter. The scrapers were copper mirrors, which had 2.25" and 2.5" outer diameters and 0.8" inner hole diameters. All the mirrors in Fig. 7 had surface figure better than 1/4 wave at 6328 Å. M_1, M_2, M_4, M_6 were quartz mirrors with aluminum coating; M_s, M_3, M_5, M_7 and M_8 were copper mirrors. All the mirrors were mounted on Aerotech precision mirror mounts that have tip and tilt knobs.

Each mirror had a specific function. M_2 and M_4 formed a confocal telescope; M_s was the reverse wave suppressor mirror, which was concave with a 2-meter radius, located 30 cm away from the reverse scraper mirror. The suppressor mirror, M_s, functioned to redirect the reverse wave back into the forward direction to achieve the reverse suppression. M_1, M_3, M_5, and M_6 were the turning flat mirrors to fold the resonator's shape, so that it could fit into the table space. The scraper mirrors, S_1 and S_2, functioned to outcouple the forward wave and the reverse wave. The outcoupled reverse wave was then sampled by using a 3"-diameter calcium fluoride (CaF_2) window as the beamsplitter. Furthermore, the sampled reverse wave was focused by using a positive lens, L_2, which had 50 cm focal length. Both L_1 and L_2 were glass

lenses which had sufficient transmittance at the operating wavelength 3.5 μm.

The gain medium was a helium-xenon gas mixture, usually used with 10 millitorr of xenon gas and 1 torr of helium gas. The laser transition was the Xe 3.5 μm line.

During the experiment, a NRC 536 pumping station and an RF Power Lab.'s linear amplifier were used. The power supply system and the laser evacuating and filling system are schematically shown in Fig. 8. The NRC 536 pumping station gave vacuum up to 10^{-7} torr. The gain medium was pumped by radio frequency power supplied by a RF Power Lab.'s model ML 500 Broadband HF amplifier. The rf amplifier can put out up to 400 watts CW at 27.5 MHz. The gain cell was a 4 cm diameter, 124 cm length cylindrical quartz tube, with calcium fluoride (CaF_2) windows on each end. The rf radiation was first input to a Drake MN2700 matching network, and then was transmitted to the gain cell through a dipole antenna. A pair of brass strips, which served as electrodes, were wraped around the gain cell and were connected to the dipole antenna. The rf energy then excited the gain medium and thus stimulated the laser transition.

Some diagnostic instruments were employed in the experiment. A Burleigh Instruments confocal Fabry-Perot interferometer model CFT-500P was used to examine the laser mode spectra. It scanned the mode spectrum by applying a ramp voltage to a PZT mounted on the fixed end mirror. The ramp voltage was supplied by a Burleigh RC-43 Ramp Generator.
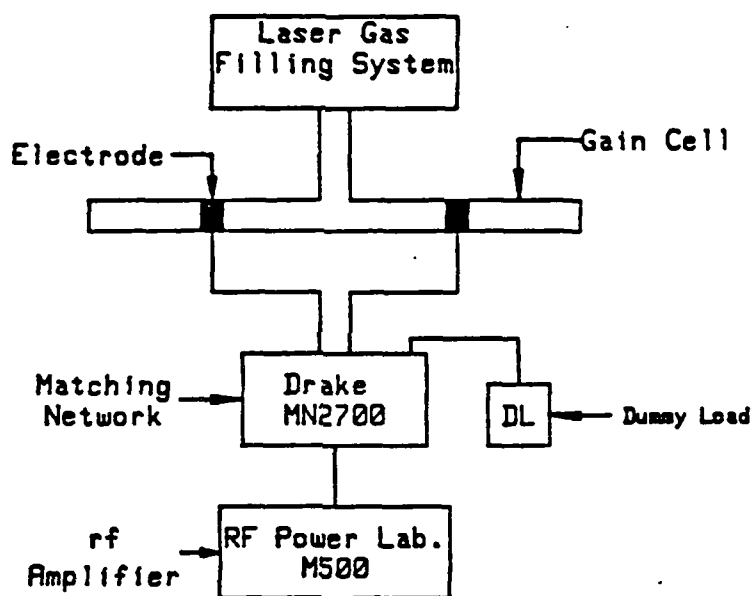
Figure 8. The laser gas evacuating and filling system, and the rf
power supply system.

The detector for the laser radiation was an indium-antimonide detector cooled to liquid nitrogen temperature. Its output was first input to a preamplifier, and then was sent to a lock-in amplifier for power measurement. An oscilloscope and a Fabry-Perot interferometer were used for mode spectrum observation.

An ISI Group infrared image camera was employed to take thermal images of forward and reverse wave intensity patterns. The image was then sent to a TV monitor and a three-dimensional image analyzer for viewing the intensity patterns.

This section concludes the discussion of the resonator and all the other equipment, which include the optical elements, the gain medium, the vacuum pump, the power supply system, and the diagnostic instruments. However, several problems with the layout and equipment were encountered when running the experiment. These problems are discussed in next section.

3.2. Experimental Concerns

The aberrations of a laser beam are undesirable because they prevent the laser beam from being focused to a diffraction-limited spot. Furthermore, as the aberrations increase, the amount of laser beam energy distributed off-axis also increases; consequently, less energy is fedback to the resonator. This lower feedback leads to a lower efficiency of the laser. Thus, the aberrations are an important concern. Furthermore, the rf noise and gas refilling problems encountered during the experiment are discussed in this section.

For the in-plane configuration as shown in Fig. 6, a program
was developed for a Hewlett-Packard desktop computer model HP9845A, to
optimize the system based on the half integer equivalent Fresnel number
consideration. During the experiment, the aberrations were minimized
by keeping the incident angles low (<4°). These minimal angles,
however, did not give a well-focused far field pattern; instead, it was
clearly astigmatic. An off-plane configuration was then used as shown
in Fig. 7. This scheme compensated the astigmatism with an increase of
coma. The compensation was achieved when astigmatism introduced in the
two axes nearly cancelled. Although the coma increased, it did not
increase as fast as the astigmatism with angle, so the coma was more
tolerable.

In addition to the aberration concern, the rf radiation that
was used to pump the active medium leaked out and interfered with every
electronic instrument. The leakage was not eliminated until the
shielding was extended to entirely enclose the matching network, the
antenna, and the gain cell with the electrodes. All the connections
were soldered. Through these efforts, the rf noise was stopped.

The gas refilling problem was encountered when the laser
stopped lasing. This problem occurred because the helium gas in the
filling pipe leaked into the pipe holding the xenon gas, thus requiring
the evacuation of the gases in the pipes and refilling with clean gases
periodically.

After solving these problems, the laser system worked well.

3.3. Optical Design [2]

In sections 3.1 and 3.2, the basic structures of both in-plane and off-plane schemes and the reason why the off-plane configuration was required, have been discussed. In this section, the resonator design equations used in the computer program and algorithm of the program, are given.

Before obtaining the desired half integer N_{eq}, it is expressed as

$$N_{eq} = \frac{a^2(M^2 - 1)}{2\lambda[ML_1 + M^2L_2 + L_3]} \qquad (26)$$

where

a = radius of the scraper hole

$L_1 = (R_2 + R_4)/2$

$M = -(R_4/R_2)$

  = geometric magnification

L = total length of the optical resonator

$$= \frac{(\text{Speed of light}) \times (\text{number of modes})}{\text{inhomogeneous linewidth of the gain medium}}$$

Since the inhomogeneous linewidth of He-Xe is about 100 MHz,

$$L = \frac{(3 \cdot 10^8 \text{ m}) \times (n)}{10^8}$$

  = 3n (meters).

Suppose we desire a 4-mode laser, then

n = number of modes = 4 ,

L = 12 meters.

The mirrors that were used have radii of curvature R_2 = 3 meters. R_4 = 4 meters.

$$M = - R_4/R_1 = - 1.33$$

$$L = \tfrac{1}{2}(3+4) = 3.5 \text{ meters.}$$

The wavelength of the laser is $\lambda = 3.5 \times 10^{-6}$ meter. To obtain the desired N_{eq}, a computer program was developed to increase L_2 or L_3 each cycle by an increment starting with zero. For each length N_{eq} was evaluated. The calculation was stopped when a value of L_2 or L_3 resulted in a value for $2 N_{eq}$ that was close to an odd integer. The significances of L_1, L_2 and L_3 are shown in Fig. 9, which is a simplification of the rings in Fig. 6 or Fig. 7.

The design that was used has L_1 = 3.5 m, L_2 = 6.4 m, L_3 = 2.1 m, a = 1.5 cm, $\lambda = 3.5 \times 10^{-6}$m. These constants make N_{eq} equal 4.5. However, the design did not result in a well-focused spot from the forward wave, so the off-plane compensation technique was employed.

The main difference between the designs depicted in Figs. 6 and 7 is the position of M_1. It was in the same plane as the other optical components in Fig. 6. Then it was changed to a position collinear with M_2 and M_3, and was higher than M_2 and M_3 in Fig. 7. This slant path introduced some astigmatism in the y-direction which compensated the astigmatism in the x-direction.

The calculated lengths, L_1, L_2, L_3, were applied to the in-plane configuration. A similar design was used in the off-plane configuration. Results are given in the next section.
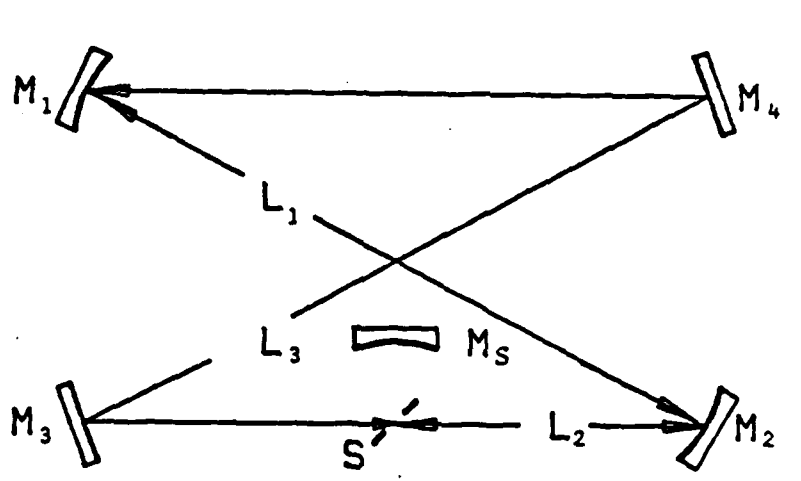
Figure 9. Simplified layout of the resonator.

3.4. Experimental Results

Reverse wave suppression by employing a suppressor mirror was
achieved in the experiment. The power measured in forward and
reverse waves, with and without the suppressor mirror, are given in
Table 1. The output power measurements with strong and weak coupling
from reverse to forward waves are also given in Table 1. The near
field and far field patterns of the foward and reverse waves are given
in Fig. 10. The comparison of the far field patterns for in-plane
scheme and off-plane schemes is shown in Fig. 11.

### 3.4.1. The Power Level Measurement and the Degree of Suppression

As shown in Table 1, the forward and reverse power levels were
measured, with and without the suppressor mirror, with and without a
germanium attenuator, at four pumping powers, 90, 100, 110 and 120
watts.

The germanium attenuator was an uncoated flat with 30% single
pass transmission, or 90% double pass attenuation at 3.5 μm. It was
inserted between the reverse wave CaF$_2$ beamsplitter and the suppressor
mirror. When the germanium flat was in, the reverse wave was
redirected back into the forward direction as weak coupling. Without
the Ge flat, the forward wave power increased with about the same
degree as the suppression of the reverse wave power at each pumping
power level except the 120 watts. After the Ge attenuator was
inserted, no power difference was observed in the reverse wave.
However, a significant amount of difference was observed with and
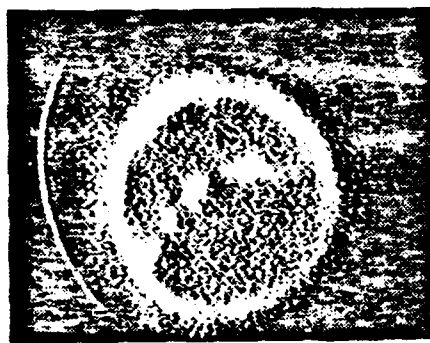without the suppressor mirror. Therefore, the weak coupling from
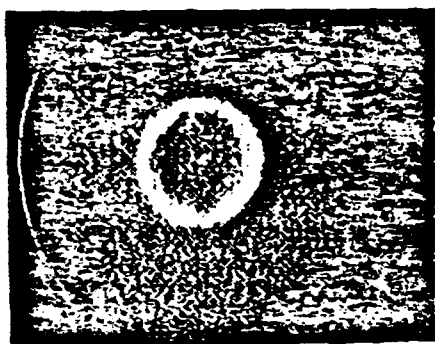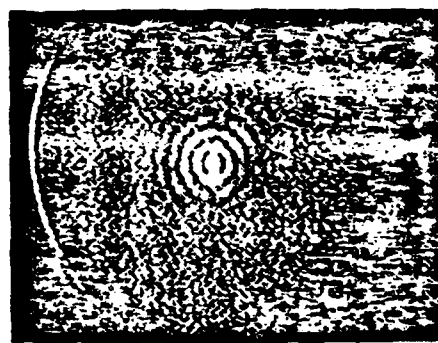
(a)

Forward wave, near field
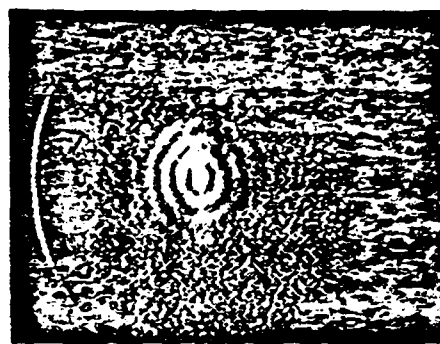
(b)

Forward wave, magnified far field

(c)

Reverse wave, near field

(d)

Reverse wave, magnified far field

Figure 10. Pictures of near field and magnified far field patterns for the forward and reverse waves.
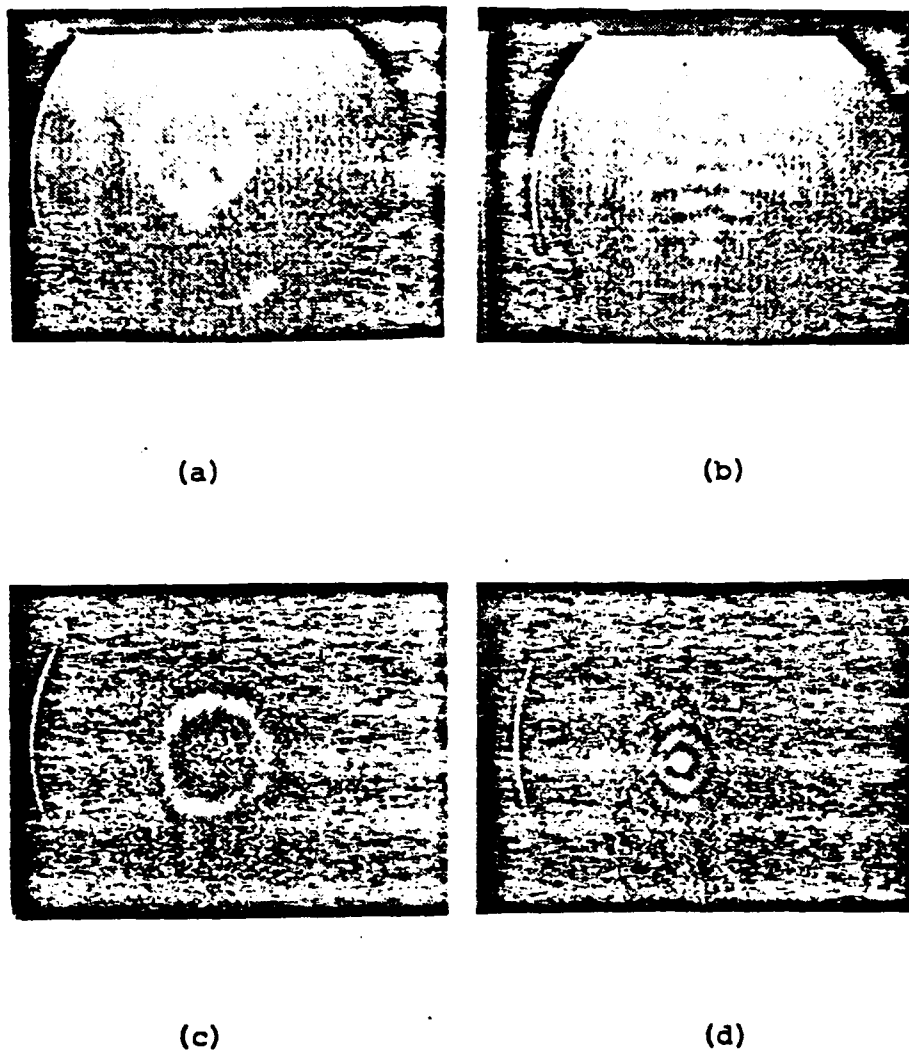
(a)

(b)

(c)

(d)

Figure 11. Comparison of field patterns for in-plane and off-plane configurations.

(a) Is the near field and (b) the corresponding far field pattterns for the in-plane ring. The corresponding patterns for the off-plane ring (c) and (d) demonstrate excellent astigmatic correction.

reverse to forward wave did not suppress the reverse wave, but added to the forward power.

The meter on the lock-in amplifier fluctuated about 10% when measuring power levels. This fluctuation indicates that the forward and reverse wave powers were drifting. Different runs of the laser usually gave different power levels at the same pumping power level. The power levels also decreased with run time. This explains why, at 110 watts pumping power, without the suppressor mirror, the forward wave power with Ge was lower than that without Ge. The forward wave power was measured at different pumping powers first, then the reverse powers at different pumping powers was measured, and as the power drifted, this might have caused the reverse wave power to be higher than the forward wave power at 110 watts pumping power. In any case, the forward and reverse wave power had about the same value, as can be seen in Table 1.

3.4.2. Near Field and Far Field Patterns

Figure 10(a-d) are the pictures of the near field and magnified far field patterns for the forward and reverse waves individually. The near field patterns of both forward and reverse waves have rather uniform intensity distributions over the annular beam. The far field patterns do not show astigmatism because of the off-plane compensation scheme.

Figure 11(a,b) shows the near field and far field patterns of the forward wave for the in-plane configuration. the magnified far field pattern was very clearly astigmatic, which demonstrates the success of the off-plane compensation scheme.

Table 1

Power levels, the degree of increase in forward wave and degree of suppression in reverse wave, with and without suppressor mirror, with strong and weak coupling.

|	Forward Wave		Reverse Wave		Pumping Power	Forward Increase	Reverse Suppression
	With Suppressor Mirror	Without Suppressor Mirror	With Suppressor Mirror	Without Suppressor Mirror			
Strong Coupling	2.000	1.280	.375	.875	90 w	56.3%	57.1%
Weak Coupling	1.280	1.280	.750	.750		0%	0%
Strong Coupling	2.400	1.520	.375	1.000	100 w	57.9%	62.5%
Weak Coupling	1.680	1.440	1.000	1.000		16.7%	0%
Strong Coupling	2.720	1.600	1.000	1.750	110 w	70 %	42.8%
Weak Coupling	1.920	1.440	1.750	1.750		33.3%	0%
Strong Coupling	3.520	2.000	1.000	1.750	120 w	76 %	42.8%
Weak Coupling	2.400	2.080	1.750	1.750		15 %	0%

3.4.3. The Mode Spectrum Measurement

Figure 12(a,b) show oscilloscope traces of the forward mode structure, obtained by using the confocal Fabry-Perot interferometer.

Figure 12(a) is a fast-scan, at 100 ms scanning time on the PZT, showing 5 repetitive peaks over the whole scan. The free spectral range of the interferometer is the range between two adjacent peaks, which is 150 MHz. Each peak had about 10 MHz half-intensity-full-width. The slanted line on the lower half of the picture was the ramp voltage applied to the PZT.

Figure 12(b) depicts a slow-scan with 5 seconds scanning time on the PZT. Slow scanning also made the ramp voltage line on the top look nearly horizontal, except for the left position, which corresponded to the fast return of the PZT. The three peaks on the bottom resulted from the fast return. The rest of the picture reveals some vague spectral information between two adjacent peaks in Fig. 12(a). The zig-zag shape may represent the fine structure of the spectrum. However, since this was not obtained with isotopically pure xenon gas, the zig-zag may be fluctuation, noise, or isotopic effects. Another scan of the laser output is shown in Fig. 12(c). A two-second scan time was used.

3.4.4. The Mode Volume Effect

The mode volumes were calculated in Chapter II, section 2.4. The reverse mode volume was 1139.2 cm^3, which was greater than the forward mode volume, 688.7 cm^3. The reason why the reverse mode volume was greater than the forward mode volume, which was contrary to what we desired, was because of the constraints imposed by the tight table
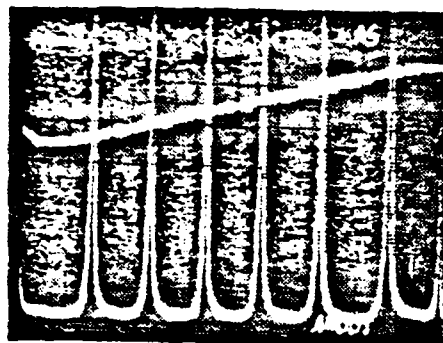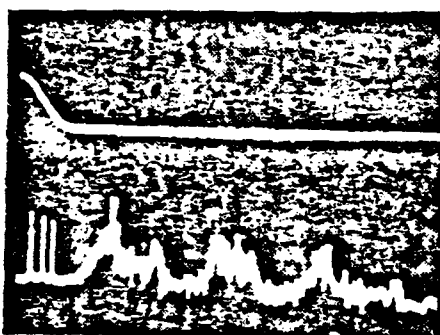
(a)

Fast scan
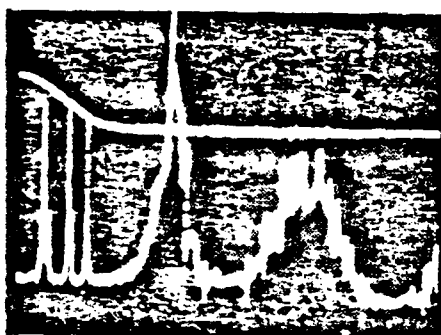
(b)

Slow scan

(c)

Medium speed scan

Figure 12. Mode spectra.

space. Nevertheless, the forward wave still had a greater output power than the reverse wave. This result, as discussed before, can be explained by the experiments results of Klüver [10], who measured the gain variation across the gain cell, as shown in Fig. 13. Klüver demonstrated that the gain was higher in the central region than near the walls of the gain cell, which had a helium-xenon gain medium with xenon 3.5 μm laser transition.

As the reverse wave was divergent along the gain cell, from Klüver's results, the reverse wave would have a portion that experienced a low gain near the wall. While the forward wave was collimated along the gain cell, with a gap between its geometric edge and the wall. This reasoning may explain why the reverse wave power was smaller than the forward wave power, even though the reverse mode volume was greater than the forward mode volume. Because it was expanding between the two scraper mirrors, some power was also lost by the reverse wave on the back of the forward scraper mirror.

The experimental results discussed above show that reverse wave suppression was achieved even though the reverse wave had a greater mode volume than the forward wave. Low order transverse far fields were observed in both the forward wave and the reverse wave. The near field intensity patterns were uniform. However, the degree of suppression was not as good as Freiberg, et al. obtained [6]. This lower degree of reverse wave suppression was probably due to the Doppler-broadened gain medium.
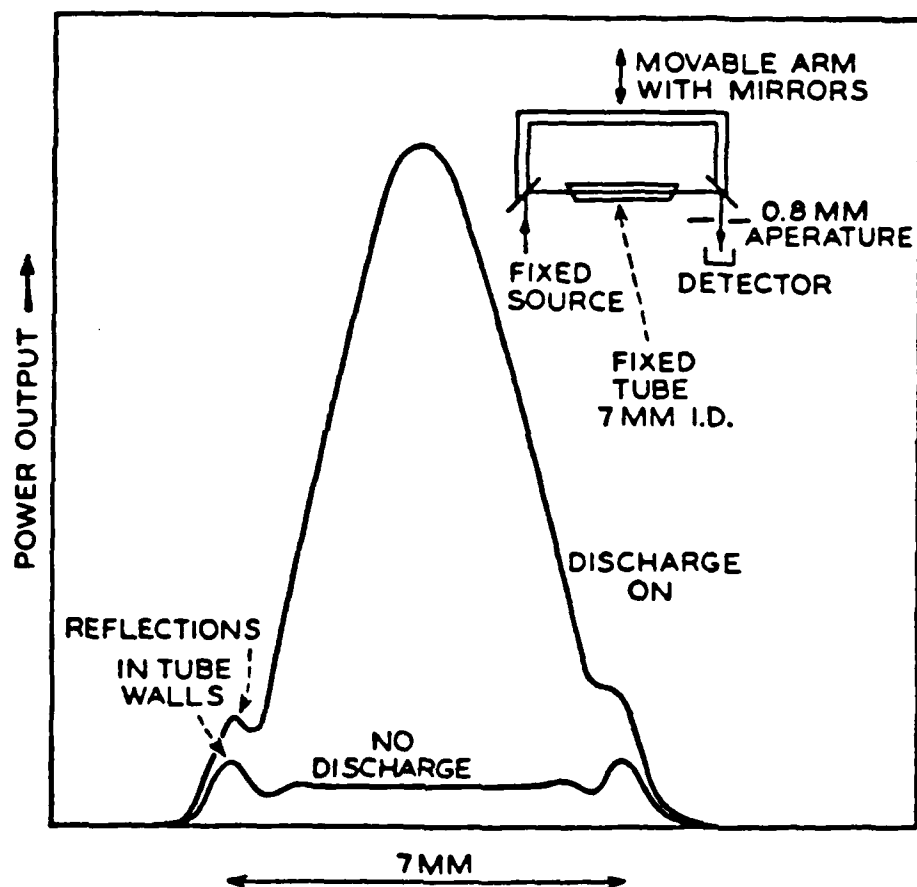
Figure 13. Gain variation across the gain cell.

CHAPTER IV

CONCLUSION

Reverse wave suppression was achieved to a certain degree in an
unstable, Doppler-broadened helium-xenon ring laser. Its degree of
suppression was 50 ~ 60%, which is much lower than that in a homoge-
neously broadened unstable CO_2 ring laser. With strong coupling from
reverse wave to forward wave, by using a 2m radius suppressor mirror,
the degree of reverse wave suppression was approximately the same as
the degree of increase in the forward wave. With weak coupling from
the reverse wave to the forward wave by inserting a germanium flat
between the CaF_2 beamsplitter and the suppressor mirror, in which the
germanium flat gave 90% double pass attenuation, the reverse wave was
not suppressed at all, and the forward wave power was increased by
about 15 ~ 30%. This increase resulted from the reverse wave power
being redirected into the forward wave. A uniformly distributed near
field pattern and a typical low order transverse mode far field pattern
were observed in an off-plane configuration, while an astigmatic far
field pattern was observed in an in-plane configuration. Although the
power measurements were obtained, the mode spectra of forward and
reverse modes were not identified, further research is desirable.
Since a numerical solution of the mode structure for an unstable,
Doppler-broadened He-Xe laser with 50 modes was done by A. H. Paxton
[11], an experiment with more modes, e.g. 10 modes or 20 modes, would

be interesting. The power measurements for a system with greater
forward mode volume would also be interesting.

REFERENCES

1. A. E. Seigman, "Unstable Optical Resonators For Laser Applications", Proc. IEEE, 53, 277 (1965).

2. W. H. Steier, "Unstable Resonators", Laser Handbook, Ed. by M. L. Stitch, 3, 3 (1979).

3. Y. A. Anan'ev, N. A. Sventsitskaya, V. E. Sherstobitov, "Properties Of A Laser With An Unstable Resonator", Zh. Eksp. Teor. Fiz., 28, 69 (1969).

4. R. J. Freiberg, P. O. Chenausky, C. J. Buczek, "CO Unstable Confocal Ring Resonators", Presented at the IEEE Int. Quantum Electronics Conf., Montreal, P. Q., Canada, May, 1972.

5. R. J. Freiberg, P. P. Echnausky, C. J. Buczek, "Unidirectional Unstable Ring Lasers", Appl. Optics, 12, 1140 (1973).

6. R. J. Freiberg, P. P. Chenausky, C. J. Buczek, "Asymmetric Unstable Traveling-Wave Resonators", IEEE J. OF QUANT. ELECT., QE-10, 279 (1974).

7. F. R. Faxvog and A. D. Gara, "Traveling-Wave Gas Lasers", Appl. Phys. Lett., 25, 306 (1974).

8. R. F. Faxvog, "Modes Of A Unidirectional Ring Laser", Opt. Letts., 5, 285 (1980).

9. A. E. Siegman, "Unstable Optical Resonators", Appl. Opt., 13, 353 (1974).

10. J. W. Klüver, "Laser Amplifier Noise at 3.5 Microns In Helium-Xenon", J. of Appl. Phys. 37, 2987 (1966).

11. A. H. Paxton, "A Preliminary Look At The Competition Of Forward And Reverse Modes In A Ring Laser", Air Force Technical Report, AFWL-TR-81-137, Air Force Weapons Laboratory, 1981; presentation given at Tri Service Chemical Laser Symposium, Albuquerque, 25 October 1982.